# Intermittent movement of localized excitations of a discrete nonlinear lattice

Benno Rumpf
*Max-Planck-Institute for the Physics of Complex Systems,*
*Nöthnitzer Straße 38, 01187 Dresden, Germany*

The movability of localized high-amplitude excitations of the discrete nonlinear Schrödinger equation is studied theoretically. The excitations are considered in connection with the surrounding low-amplitude waves. Migrating localized excitations undergo a temporary change of their content of the quantities that are conserved by the system's dynamics. Such fluctuations are caused by the interaction of excitations with surrounding low-amplitude waves. This requires the rare event of an intermediate decrease of the system's entropy, which is the statistical reason for the pinning of these structures at the lattice.

PACS numbers: 63.20.Pw,64.60.Cn,45.05.+x,42.65.Jx

## INTRODUCTION

This paper explores the movability of localized excitations in the discrete nonlinear Schrödinger equation. High-amplitude localized excitations that emerge spontaneously from a background of low-amplitude waves are a dynamical property of many spatiotemporal systems. Examples for this are collapses in plasmas and Bose-Einstein condensates or the self-focusing of light in Kerr-nonlinear media. In arrays of coupled optical fibers [5], the self-focusing dynamics increases the light intensity within a few fibers, and decreases the intensity in all other fibers. The envelope of the field in a nonlinear fiber array (indexed by $n$) with a zero group velocity dispersion is governed [4] by the the discrete nonlinear Schrödinger equation (DNLS)

$$i\frac{\partial \phi_n}{\partial t} = \phi_{n+1} + \phi_{n-1} + |\phi_n|^2\phi_n \qquad (1)$$

where the 'time' $t$ means the normalized propagation distance. The modulus-square norm (or 'particle number') $A = \sum \phi_i\phi_i^*$ is a conserved quantity of this equation. Equation (1) derives as $i\dot{\phi}_n = \frac{\partial H}{\partial \phi_n^*}$ from the Hamiltonian (or 'energy') $H = \sum_i(\phi_i\phi_{i+1}^* + \phi_i^*\phi_{i+1}) + \frac{1}{2}\phi_i^2\phi_i^{*2}$ which is another conserved quantity. An interesting phenomenon in this spatially discrete system is the trapping of intensity-peaks in the fibers: Highly localized solutions interact most strongly with the discrete structure of the supporting optical medium, so that they are pinned at the lattice for most of the time and rarely migrate to a neighboring lattice site. This is shown in a simulation (Fig.1a,b) where the DNLS with $N = 1024$ lattice sites and periodic boundary conditions has been integrated with spatially homogeneous low-amplitude initial conditions $\phi_n(t = 0) = 0.2$. This homogeneous state is phase-unstable, and within a few hundred time units several localized high amplitude structures emerge from a disordered low-amplitude background at most lattice sites. Fig.1a shows the rare event of a migration of a localized localized from one lattice site to a neighboring lattice site. It shows the profile of the squared amplitude $|\phi_n(t)|^2$ as a function of time (from 1058 time units till 1073 time units after the beginning of the integration) in a small segment (11 lattice sites) of the chain. It shows that at first a high amount of particles (up to $|\phi_{125}|^2 \approx 4.5$) is gathered at the site 125, but at $t \approx 1066$ these particles move to the neighboring lattice site 126 within 3 time units. The particle density decays rapidly with the distance from the peak to the level $|\phi|^2 \sim \mathcal{O}(0.04)$ of the surrounding disordered waves.

The interaction with these low-amplitude waves is crucial for the migration, and high-amplitude excitations are pinned to the lattice when all oscillators except those in the close vicinity of the peak are set to zero. This connection of the pinning of an excitation and low-amplitude waves is studied in a second numerical experiment with equation (1) for a chain of 512 lattice sites (Fig.1c). The

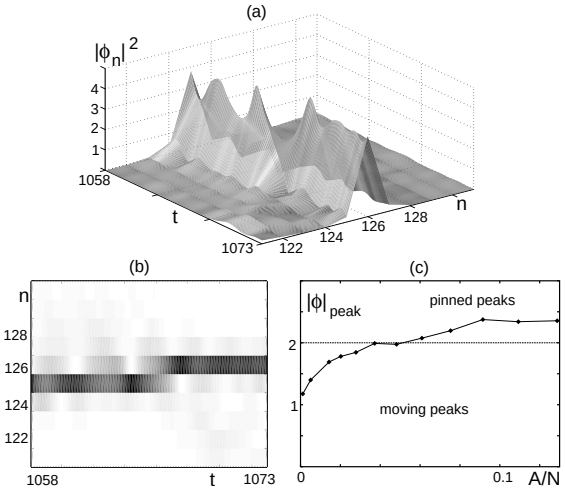


FIG. 1: (a) Particle density $|\phi_n(t)|^2$ in a sector of 11 lattice sites from a chain of 1024 lattice sites. The sector shows a small time interval of 15 time units at which a migration occurs out of a long integration time. (b) The same sector as (a), where dark gray means a high particle density $\phi_n|^2$. (c) The maximum height $|\phi_n|$ of peaks that are found to migrate as a function of the particle density $A/N$ of the surrounding low-amplitude waves.

initial condition is a single isolated excitation in an environment of low-amplitude random waves with a white spectrum where all wavenumbers have the same power. This system is integrated over 10,000 time units for various peak-heights and wave-amplitudes and to observe whether the excitation migrates or not. The lattice-pinning turns out to be stronger if the amplitude of the excitation is higher. Fig.1c shows the time-average amplitude $|\phi|_{peak}$ of the highest localized structure that has been found to migrate at least once during the 10,000 time units of the integration as a function of the surrounding low-amplitude waves. The probability of a peak to migrate decreases rapidly with its height, and the threshold for the pinning of peaks is about $|\phi| \approx 2$, increasing slightly with the level of the surrounding disordered waves. Peaks that are higher than the one of Fig.1a,b are usually pinned at one site.

The reason for this pinning effect and its possible applications in optical signal switching have been investigated in many papers. Unlike continuous systems whose solitary solutions can move without change in shape, solutions of discrete systems have no Goldstone mode so that their shape changes when they propagate in space. In the generic case of a nonintegrable lattice dynamics, no analytic solution schemes for moving solutions are available, and numerically observable solutions radiate low-amplitude waves as they propagate through the lattice. The dynamics of solitary long-wave solutions is well approximated by a continuum description, but high-amplitude excitations with a width of the order of the lattice constant are subjected to a strong periodic force that impedes their movement. Known stable solutions of the DNLS are statically pinned to the lattice. One approach to capture this feature uses the concept of the Peierls-Nabarro barrier that originally describes how the periodic lattice potential of crystals prevents the migration of defects unless some external force exceeds a threshold value. This approach [3] asserts that the migration occurs via an intermediate state with a different energy content. This effective pinning energy however is not a fixed barrier caused by the lattice as it generically depends on the amplitude of the excitation itself [7]. It has been pointed out [6] that this approach assumes the conservation of the action during the migration. Alternative paths with intermediately changing amplitudes could migrate without any change of energy. Hence the amount of particles and energy that are locally absorbed this structure are crucial both for pinning and for migrations of localized excitations.

This paper explains the pinning and the possibility of migrations of localized excitations interacting with low-amplitude waves as a statistical process. It makes use of the recent progress of the understanding of localized solutions as statistical phenomena [8],[9]. Localized excitations must be seen in connection with surrounding low-amplitude waves. Depending on the temperature of these waves, the excitations can grow or they can be melted away. This approach derives the amounts of energy and particles in the localized excitations from the thermodynamic potentials of surrounding low-amplitude waves. This yields a *local* conservation of both quantities within the excitation on longer time scales, while they fluctuate on short scales.

First, this paper shows that the trajectory of migrations can be described by an idealized dimer model that reduces the lattice to two sites. This migrational orbit exists only for peaks below a certain critical energy. Above this threshold, the energy conservation prevents any migration of peaks.

Second, the total lattice is considered and the width of the localized excitations is taken into account. Perfect localized excitations with no suurounding low-amplitude waves are always pinned and they cannot migrate spontaneously, but migrations can be triggered by an interaction with surrounding low-amplitude waves. A migration to a neighboring lattice site requires an intermediate state that is statistically unfavorable. Only huge random fluctuations of its particle- and energy-contents allow the peak to move to a neighboring site.

Most figures (Fig.1a,b, Fig.2a,b, Fig.3b, Fig.6, Fig.8, Fig.9) derive from one numerical simulation of a migration in equation (1). It has been confirmed in many more simulations that this process of migration is representative.

## LEVEL-SETS AND THE PATH OF THE MIGRATION

### Conservation laws during the migration

Fig.1 indicates that there is a high particle density during the migration only at the two lattice sites $n = 125$, the initial location of the peak, and at $n = 126$, its location after it has moved. Fig.2a shows the evolution of the particle numbers at these two lattice sites during the migration. The particle number at the site 125 decreases from $|\phi_{125}|^2 \approx 4.6$ to a value close to zero. Simultaneously, the particle number at the neighboring site 126 increases from around zero to $|\phi_{126}|^2 \approx 4.5$. The total number of particles at the two sites is almost constant $|\phi_{125}|^2 + |\phi_{126}|^2 \approx 4.6 \pm 0.1$, and there is little exchange of particles of these two lattice sites with their neighbors where the amplitudes remain small during the migration. The migration is basically a transfer of particles from the 'donor' lattice site 125 to the neighboring 'acceptor' site 126. Corresponding to the growth and decay of the adjacent peaks, the nonlinear energy $|\phi_{126}|^4/2$ grows and $|\phi_{125}|^4/2$ decays (Fig.2b). Unlike the particle number, the sum of these two nonlinear energy contributions is not conserved and it decreases intermediately during the migration. The energy that is released

from the nonlinearity is stored in the central bond so that the coupling energy $2Re(\phi_{125}\phi^*_{126})$ grows intermediately (Fig.2b). The sum $|\phi_{125}|^4/2+|\phi_{126}|^4/2+2Re(\phi_{125}\phi^*_{126})$ of the nonlinear energies at the two sites and the coupling energy in the central bond is roughly conserved.
This approximate local conservation of energy and particles at two sites suggests to model the migration process by a perfectly isolated dimer of only two oscillators $\phi_l$ and $\phi_{l+1}$, with a constant particle number

$$A_d = |\phi_l|^2 + |\phi_{l+1}|^2 \tag{2}$$

and a constant energy that includes the nonlinear contribution from the two sites and the energy from the central bond

$$\begin{aligned} H_d &= \tfrac{1}{2}|\phi_l|^4 + \tfrac{1}{2}|\phi_{l+1}|^4 + 2Re(\phi_n\phi_{l+1}) \\ &= \tfrac{1}{2}|\phi_l|^4 + \tfrac{1}{2}|\phi_{l+1}|^4 + 2|\phi_l||\phi_{l+1}|\cos\alpha \end{aligned} \tag{3}$$

where $\alpha$ is the phase difference between $\phi_l$ and $\phi_{l+1}$. This model neglects smaller fluctuations of the dimer's energy and particle content due to interactions with the surrounding low-amplitude oscillators.

### Intersection of level-sets

Writing the donor as $\phi_l = |\phi_l|e^{i(\psi-\alpha/2)}$ and the acceptor as $\phi_{l+1} = |\phi_{l+1}|e^{i(\psi+\alpha/2)}$, the four-dimensional phase space of the dimer can be represented by the three coordinates $|\phi_l|$, $|\phi_{l+1}|$, $\cos\alpha$, plus the trivial phase variable $\psi$. The two conservation laws define level sets in the phase space.
Any solution conserving (2) and (3) is restricted to the intersection manifold of the two level sets, which determines the path of the migration. Parameterized by $\nu \in [0,1]$, this onedimensional manifold is given by

$$\begin{aligned} \phi_l(\nu) &= r\sqrt{1-\nu}\,e^{i(\psi-\alpha/2)} \\ \phi_{l+1}(\nu) &= r\sqrt{\nu}\,e^{i(\psi+\alpha/2)} \end{aligned} \tag{4}$$

with $\cos\alpha = r^2\sqrt{\nu-\nu^2}/2$. It connects the state ($|\phi_n(\nu=0)| = r$, $|\phi_{n+1}(\nu=0)| = 0$) before the migration, when all particles are gathered at the site $n$, and the state after the migration ($|\phi_n(\nu=1)| = 0$, $|\phi_{n+1}(\nu=1)| = r$), when all particles are gathered at $n+1$. Fig.3a shows the level sets of $A_d = 4$ and $H_d = 8$. Their intersection set includes the initial state $|\phi_l(\nu=0)| = 2, |\phi_{l+1}(\nu=0)| = 0$. This intersection path closely matches the numerical trajectory. Fig.3b shows the intersection line of the level sets and the trajectory of the migration of the simulation of Fig.1. The numerical data are given as points with distances of 0.1 time units. It also shows the projections of the data to the three planes $\cos\alpha = 0$, $|\phi_{125}| = 0$, $|\phi_{126}| = 0$.
Corresponding to the solution (4), the particle number of the initial peak $|\phi_l|^2 = r^2(1-\nu)$ decays linearly as a function of $\nu$, while it grows as $|\phi_{l+1}|^2 = r^2\nu$ at the

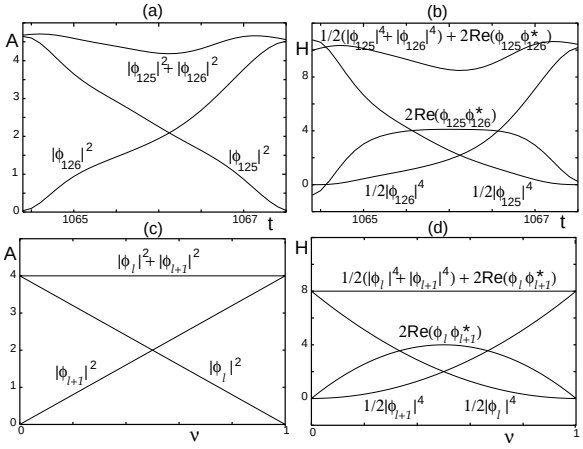


FIG. 2: Particle number $|\phi_{125}|^2$ and $|\phi_{126}|^2$ (a,c) and nonlinear energies $|\phi_x|^4/2$, $|\phi_x|^4/2$ and coupling energy $2Re(\phi_{125}\phi^*_{126})$ (b, d) during the migration. The numerical data (a),(b) describe the the migration of Fig.1a,b as a function of time for $(1064.4 \le t \le 1067.5)$. The analytical data (c),(d) are functions of the parameter $\nu$ (see equation (4).

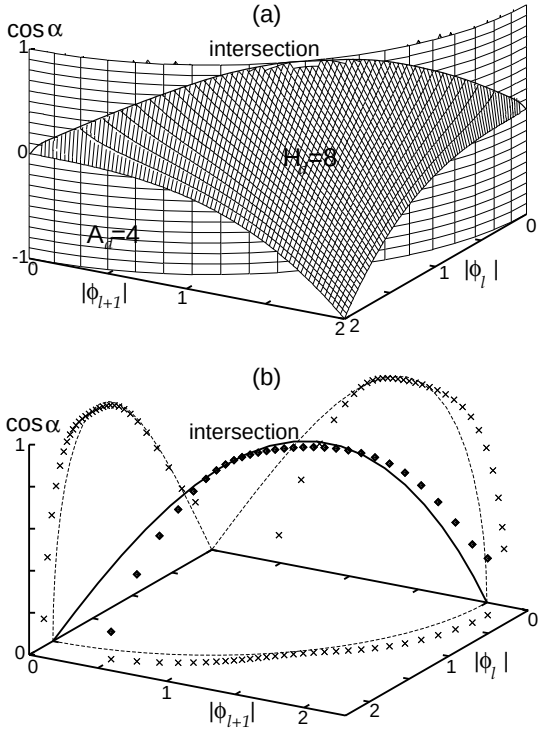


FIG. 3: (a) Level sets of $A_d$ and $H_d$ for a peak height $|\phi| = 2.0$ as functions of $|\phi_n|$, $|\phi_{n+1}|$, $\cos\alpha$. (b) Intersection of the level sets for $|\phi| = 2.0$ (line) and the trajectory of the peak migration from the simulation of Fig.1 (points). The time interval is $[1064.5, 1067.5]$, the interval between subsequent points is 0.1 time units. The dotted lines and the crosses are the projections to the level sets $|\phi| = 0$ and $\cos\alpha = 0$.

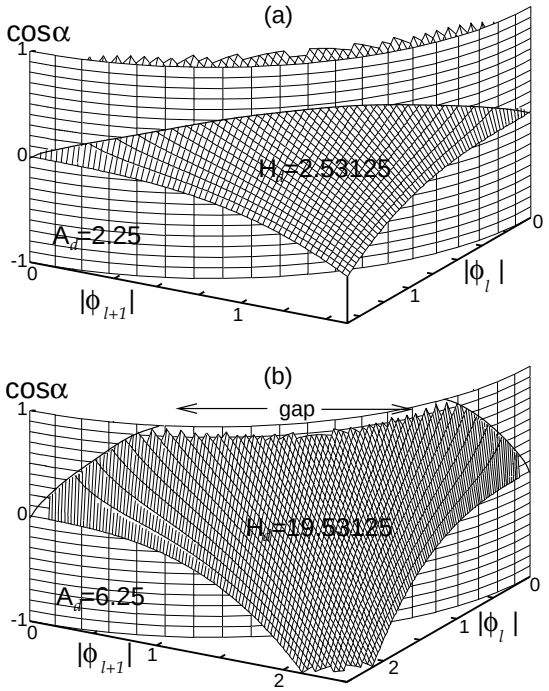


FIG. 4: Level sets of $A_d$ and $H_d$ for peak heights (a) $|\phi| = 1.5$ and (b) $|\phi| = 2.5$. For the higher initial peak (b), there is no closed connection between $|\phi_n| = 2.5, |\phi_{n+1}| = 0$ and $|\phi_n| = 0, |\phi_{n+1}| = 2.5$ on the intersection set.

neighbor site (Fig.2c). Similarly, the nonlinear energies decay and grow as $r^4(1-\nu)^2/2$ and $r^4\nu^2/2$ respectively, while the bond between the two sites stores the energy $r^4(\nu - \nu^2)$ intermediately (Fig.2d). These particle- and energy densities as functions of the parameter $\nu$ closely agree to the numerical data (Fig.2a,b).

### Threshold of the migration

Fig.4a shows the intersection path that connects a donor $|\phi_l(\nu = 0)| = 1.5$ with an acceptor $|\phi_{l+1}(\nu = 1)| = 1.5$. Fig.4b shows that there is no such closed connection for $|\phi| = 2.5$. The closed connection (4) exists only if the condition $\cos\alpha \leq 1$ is fulfilled for all $\nu \in [0, 1]$. With its maximum $\cos\alpha(\nu = 1/2) = r^2/4$ at the migrations midpoint $\nu = 1/2$, this inequality is only fulfilled if $r^2 \leq 4$, which corresponds to an initial donor peak amplitude $|\phi(\nu = 0)| \leq 2$.

Peaks with $|\phi| > 2$ cannot migrate, since the $|\phi|^4$-energy of the initial peak cannot be stored in the coupling term $2Re(\phi_l\phi^*_{l+1})$ at the midpoint of the migration. From the particle conservation it follows that the amplitudes of the two oscillators are $|\phi_l(\nu = 1/2)| = |\phi_{l+1}(\nu = 1/2)| = r/\sqrt{2}$ at this point. Such a state of two isolated peaks with a central bond ('isolated bond' or 'ib' in Fig.5) can maximally absorb the energy $H = r^4/4 + r^2$ for $\alpha = 0$, or a smaller amount of energy for a nonzero angle $\alpha$. A single isolated peak ('ip' in Fig.5) has an energy $H = r^4/2$. Fig.5 shows that the maximum energy of the central-bond state is larger than the energy of the isolated peak for $A < 4$. In this range a central bond state with a suitable $\alpha$ can absorb the energy of the initial isolated peaks. In contrast, the energy of the isolated peak with $A > 4$ is higher than the energy of any intermediate central-bond state, and the local conservation laws (2) and (3) are incompatible with a migration.

The limit for large $a$ corresponds to the original argument [3] for the Peierls-Nabarro barrier in the DNLS: For an initial donor amplitude $|\phi_l| = r$, the amplitudes of donor and acceptor will match as $|\phi_l| = |\phi_{l+1}| = r/\sqrt{2}$ at the time when half of the particles are transfered. For $r$ large, the quadratic coupling energy can be neglected in comparison to the quartic nonlinear energy. The energy $H_4 = r^4/4$ of this state differs from the initial energy $H_4 = r^4/2$, and the difference between these two energies may be regarded as a Peierls-Nabarro barrier that pins the peak at one site.

### Dynamics of the migration

The intersection line between the two shells $A = const$ and $H = const$ is an exact solution of a migration of a peak from the site $l$ to $l + 1$ in the dimer model [1], [2]. Its dynamics is governed by

$$\begin{aligned} i\dot{\phi}_l &= \phi_{l+1} + |\phi_l|^2\phi_l \\ i\dot{\phi}_{l+1} &= \phi_l + |\phi_{l+1}|^2\phi_{l+1} \end{aligned} \tag{5}$$

These equations are obviously integrable and can be solved analytically [1], [2] and the solution reproduces the the intersection path of $A = const$ and $H = const$ as

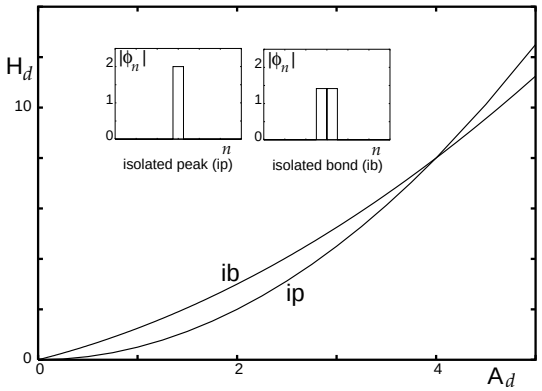


FIG. 5: Energy versus particle number of an isolated peak (ip) and of two isolated peaks with a central bond (ib). The dimer energy of both excitations match when the particle-number of the dimer is $A_d = 4$.

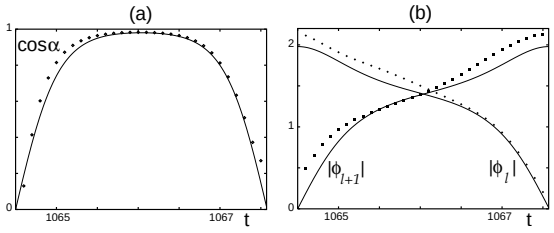


FIG. 6: (a) $\cos\alpha$ and (b) $|\phi_n|$ and $|\phi_{n+1}|$ as functions of time during the simulation of Fig.1 (points) and for the analytic solution of the two-site model with $r = 1.96$ (lines) as functions of time.

a function of time. The solution of the equations (5) is

$$\begin{aligned} |\phi_l| &= r\sqrt{(1+\mathrm{cn}(2t, r^2/2))/2} \\ |\phi_{l+1}| &= r\sqrt{(1-\mathrm{cn}(2t, r^2/2))/2} \\ \cos\alpha &= \tfrac{r^2}{4}\mathrm{sn}(2t, r^2/2) \\ \sin\alpha &= -\mathrm{dn}(2t, r^2/2) \end{aligned} \tag{6}$$

while $\psi$ has the constant speed $\dot{\psi} = 3r^2/4$. This is exactly the intersection path (4) where $\nu(t) = \frac{1}{2}(1-\mathrm{cn}(2t, r^2/2))$ has been determined. Fig.6 shows that $|\phi_l|$ decays monotonically from $r$ to 0 while $|\phi_{l+1}|$ grows. $\cos\alpha$ increases from 0 to its maximum $r^2/4$ and decays to 0 subsequently, which is only possible if the initial amplitude is $\sqrt{a} \leq 2$. $\alpha$ grows from $-\pi/2$ to a value that is less or equal 0 and decays again to its initial value. The solution of (6) is very close (Fig.6 where $r = 1.96$) to the numerical data from the simulation of Fig.1.

## FLUCTUATIONS AND MIGRATIONS OF THE EXCITATION

The two-site model neglects all energy- and particle contributions except for the donor and the acceptor site, which leads to a qualitative shortcoming of this idealized description of peak-migration in the DNLS equation: The orbit (6) that connects the two localized excitations of the dimer is *periodic* in time, while sufficiently high ($r > 1$) localized excitations of the full DNLS chain are pinned at one lattice site, before its particles are shifted suddenly to a neighboring lattice site where the excitation is again pinned for a long time. It is necessary to investigate the interactions between the peak and its low-amplitude environment to explain why the peak is locked at one lattice site for most of the time and why it can suddenly move to a neighboring site.

### Stationary excitations and breathers

Excitations that are stationary in a frame rotating with the frequency $\omega$ are solutions of

$$0 = \phi_{n+1} + \phi_{n-1} + |\phi_n|^2\phi_n + \omega\phi_n \tag{7}$$

Reading this set of equations as a map $(\phi_{n-1}, \phi_n) \to (\phi_n, \phi_{n+1})$ with the lattice-site index $n$, localized excitations correspond to heteroclinic orbits connecting the fixed points $\phi_{-\infty} = 0$ and $\phi_{+\infty} = 0$. Equation (7) is equivalent to the condition

$$0 = \frac{\partial}{\partial\phi_n^*}(H + \omega A)$$

for extrema or saddle points of the energy where the Lagrange parameter $\omega$ constrains the particle number $A$. One well-known localized real solution of (7) is site-centered, i.e. the amplitudes decay symmetrically at the left and the right of the site with the maximum amplitude (solution cp in Fig.7). This central-peak solution is stable, as it has a maximum of energy for a given particle number. Central-peak solutions at different lattice sites correspond to different elliptic fixed points in phase space. There is no path connecting these islands while conserving both energy and particle number, and a perfect central-peak solution will not move at all. However, such a migration might proceed along a path in phase space where energy and particle number are not conserved if some external force changes these two quantities temporarily. The deviation from the original amount of these quantities is maximal at the midpoint of the migration, where $l$ and $l+1$ have the same amplitudes, and the solution has the shape of the solution cb in Fig.7. This unstable solution of (7) is a saddle-point in the energy under the constraint of fixed $A$. It has a lower energy (line cb in Fig.7) than the site-centered solution (line cp in Fig.7) with the same particle content. Assuming a migration conserves $A$ but not $H$, the energy has to decrease at least to the line cb intermediately. Alternatively, the line cb can also be reached by increasing the particle number temporarily. Any migration path requires a change of either energy or particle number that bridges the gap between the lines cp and cb. Alternative migration paths that do not pass through the central-

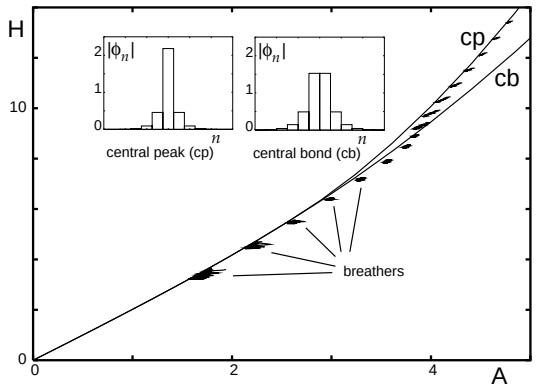


FIG. 7: Energy versus particles for the stationary central-peak (cp) solution and the central-bond (cb) solution (lines) and for breathers with various heights (points).

bond state have to overcome an even larger gap.
This gap impedes the migration of central-peak solutions for all values of $A$ and the excitation cannot overcome the gap spontaneously without an external cause. This energy- and particle-balance concerns the localized excitation as a whole, while the gap obtained in Fig.5 concerns only the central two lattice sites. Fig.5 and Fig.7 yield independent conditions for a migration: At some point during the migration, the energy of the central two oscillators has to be below the line ib of Fig.5, while the energy of the broader structure has to be below the line cb of Fig.7.
This gap is smaller for 'breather' solutions which have an energy slightly below the line cp. These solutions are similar to the central-peak solution, but their amplitude has a 'breathing' behavior corresponding to periodic orbits close to the elliptic fixed point that represents the site-centered solution. Fig.7 shows the energies and particle numbers of breathers that emerge from an initial condition with a peak at one lattice site and a zero amplitude everywhere else. The total energy of this central site and the six neighbors at its left and its right are plotted for 100 integration steps of 0.25 time units each. It turns out that breathers with particle numbers up to $A \approx 4$ have a lower energy than a central-bond solution with the same particle number, and they are more likely to migrate.

### Statistical nature of localized excitations

In a recent paper [9] it has been shown that localized excitations in the DNLS equation are *statistical* phenomena that emerge naturally for a great variety of initial conditions. The DNLS equation is a non-integrable Hamiltonian system, and its solutions can be understood from the statistical ensemble related to its two conserved quantities. Its analysis shows that its state of maximum entropy for many cases ($E > 0$ and $A/N$ small) consists of low-amplitude waves at almost all lattice sites, and only at a few scattered high-amplitude excitations. In this state, the low-amplitude waves absorb the amount $E_<$ of energy and $A_<$ of particles, while the peaks absorb the amounts $E_>$ and $A_>$. The sums $E = E_< + E_>$ and $A = A_< + A_>$ are the total conserved quantities. The system's total entropy has two contributions, one from the low-amplitude waves,

$$S_< = N \ln(\frac{4A_<^2 - E_<^2}{4A_< N}) \qquad (8)$$

and one from the localized high-amplitude excitations $S_>$. It turns out that $S_<$ yields the bulk of the entropy provided that the system has a low particle-density $A/N$. The maximum of the total entropy corresponds to a state where the low-amplitude waves absorb nearly all particles $A_< \approx A$, but have an energy that is close to zero $E_< \approx 0$. In the same time, the peaks absorb any surplus of energy $E_> \approx E$ using a minimum amount of particles. The central-peak solution is the thermodynamically 'ideal' excitations since it absorbs more energy than any other solution using a given number of particles. The temperature and the chemical potential of the waves maintain the excitations of this type. This thermodynamic force leads to a *local* approximate conservation of the amount of energy and particles in each of the excitations.

### Fluctuations causing a migration

Localized solutions randomly exchange particles with the embedding low-amplitude waves, so that the particle and energy contents of the localized excitations is not constant, but fluctuates constantly. The energy of the low amplitude waves is zero in the equilibrium, and their entropy reduces by

$$\Delta S_< = -\frac{\partial S_<}{\partial A}|_{E=0} \Delta A = -N \frac{\Delta A}{A}$$

if $\Delta A$ particles are transfered to the localized excitations. Huge particle transfers are rare since huge fluctuations of the entropy are rare. These fluctuations are one of the possible forces that can allow the localized structure to bridge the gap between its initial energy and particle number and these quantities at an intermediate stage during the migration. Fig.8 compares the fluctuating amount of energy and particles (irregular line) in the localized excitation from Fig.1 with the energy and particles of stationary central-peak and central-bond excitations (the lines cb and cp are the same as in Fig.7). In Fig.8b, the energy and particle contents of the excitation is measured in a patch of 13 lattice sites with the peak at the center in a period of 60 time units at the migration. The energy content changes relatively little compared to the particle number, which is due to the low energy of the low-amplitude waves. The energy-particle trace of

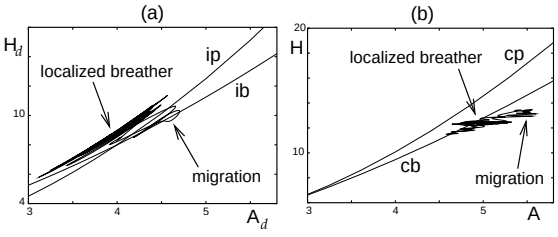


FIG. 8: Trace of the energy versus the particle number of the excitation of Fig.1 over 25 time units during the migration. (a) shows the energy and particles of only the two central lattice sites 125 and 126, (b) shows these quantities measured in a broader patch of 13 lattice sites. The lines ip,ib,cp,cb are the same as in Figs.5 and 7.

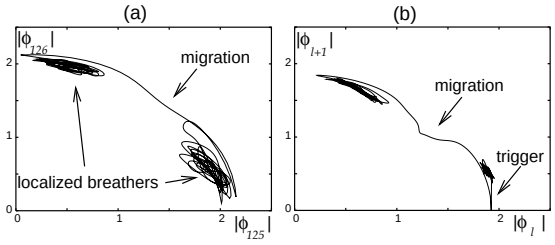


FIG. 9: (a) $|\phi_{126}|$ versus $|\phi_{125}|$ for the migration of Fig.1. (b) A similar migration that is triggered by externally setting the acceptor amplitude $|\phi_{l+1}|$ to zero at one point during the numerical integration.

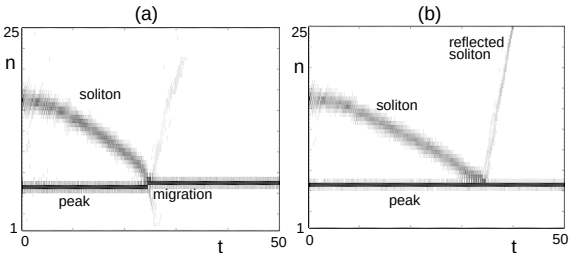


FIG. 10: (a) Collision of a peak with the height $|\phi| = 1.95$ with a soliton resulting in a migration of the peak by one lattice site. (b) Collision of a peak with the height $|\phi| = 2.35$ with a soliton leads to no migration.

the excitation is in the region of the central-bond solution (line cb), well below the line cp for the stationary central-peak solution. For a migration, the trace has to be below the line cb, which is the case for much of the time. The actual migration corresponds to the largest temporary increase of the particle number, which reaches $A = 5.5$ for a short time.

In addition to this condition on the total energy and particle number of the excitation, enough particles need to be available in the center of the excitation during the migration. Fig.8a gives the energy and particles of the donor and the acceptor site and the central bond in comparison to the lines ip and ib of the dimer of Fig.5. Again, a migration is only possible if the trace of the excitation is below the line ib. Unlike Fig.8a, this is not fulfilled for most of the time and the line cb is crossed only for a short time during which the migration actually takes place. This barrier from the center of the excitation is the one that is more difficult to overcome.

This explains pinning and migration of peaks as statistical processes: Depending on the gap between the lines cp and cb as well as ip and ib, an amount $\Delta A$ of particles has to be transfered from the fluctuations to the coherent excitation. This amount is smaller for breathing peaks with a lower energy per particle (Fig.7). The gap of particles between the site-centered excitation and the bond-centered excitation increases with the height of this excitation, while it is smaller for breathing peaks that have a lower energy. Migrations become less likely with the height of the peak as this would require a huge and unlikely fluctuation in its content of particles. On the other side, the probability of such fluctuations increases with the amplitude of the waves in the background (Fig.1c).

Fig.9a shows the trace of $(|\phi_l(t)|, |\phi_{l+1}(t)|)$ during the migration of Fig.1. Before the migration, most particles are gathered at the site $l$ with $(|\phi_l(t)| \approx 2)$, while the amplitude at $l+1$ is small and the amplitudes at both sites fluctuate irregularly. Then, following a short-lived increase of the amplitude at $l$, the particles migrate to $l+1$. The localized excitation is trapped at this new site until another huge fluctuation allows it to move again.

The migration orbit can be understood as a heteroclinic connection of the two tangles representing localized excitations. The migration starts when the trajectory accidentally approaches this orbit, which requires a sufficiently low energy and high particle number. During the migration when $|\phi_l|$ and $|\phi_{l+1}|$ both are larger than their neighbors, this orbit is well approximated by the dimer orbit (6). As it approaches the acceptor site the interaction with low-amplitude waves is again important and the the trajectory leaves the dimer orbit. The final state is again a tangle at $l+1$.

### Trigger of migrations

Migrations can be triggered externally by setting the trajectory at a the starting point of the heteroclinic connection, rather than waiting for the system to reach this point accidentally. This is shown in Fig.9b where the localized excitation rests at the site $l$ when $\phi_{l+1}$ is suddenly set to zero. This reduces the energy of the central bond and the system is at the starting point of the dimer orbit (6), so that it migrates and becomes entangled at $l+1$ in a way that is similar to the migration caused by random fluctuations of Fig.9a.

An alternative way of triggering a migration is to change the phase of the acceptor site. The phase difference of the donor and the acceptor is $\pi/2$ at an early stage of the dimer solution (6), while the phase difference of the central peak and its neighbors is zero for the central-peak solution cp (Fig.7). Changing the phase of one of the neighbors by at least $\pi/2$ turns this site to an acceptor, so that the peak migrates. This however reduces the energy of the excitation after the migration.

Another possibility to trigger a migration is the collision with a low-amplitude solitary wave. These solitons can be produced by exciting a few neighboring oscillators, and they can also occur in not fully thermalized low-amplitude waves (e.g. in the simulation of Fig.1). Such a wave provides particles with a low energy content locally to the the peak which can allow the peak to cross the lines ib and cb so that it enters the domain where it can move. This triggers migrations more efficiently than in-

teractions of the peak with low-amplitude random waves. Fig.10 shows the impact of such collisions for peaks with two different heights. The lower peak $|\phi| \approx 1.95$ moves by one lattice site after the collision. The higher peak $|\phi| \approx 2.35$ remains at the lattice site, and the solitary wave is reflected. Due to its height, the gap between the lines ip and ib and between cb and cp are larger than the amount of particles provided by the low-amplitude soliton. The amplitude of the peak increases in either case, as both energy and particles are absorbed from the incoming soliton. The reflected or transmitted solitons carry the surplus of these quantities, therefore the collision changes their shape and speed.

## CONCLUSIONS

The effect of lattice-pinning of excitations depends on the amount of the two quantities $H$ (energy) and $A$ (particles) that they absorb locally. High-amplitude excitations with a high ratio of energy per particle cannot move as this would require intermediate changes of this ratio whenever the excitation has its center between two adjacent lattice site.

The energy- and particle balance of these migrations has been considered in two different ways, firstly only for the two sites (donor and acceptor) with the highest amplitude during the migration, secondly for the broader structure of the excitation including adjacent sites with lower amplitudes. The simple model of only two sites gives a threshold beyond which no continuous migration path for localized excitations exists (Fig.5). Below this threshold, the trajectory of the migration can be computed analytically (Fig.3). Within a short period of time most of the particles move by one lattice site, while the total particle number in the dimer remains almost constant (Fig.2). The energy and particle balance for the broader region of the excitation gives site-centered excitation (cp in Fig.7) as stable solutions of the DNLS. No path conserving both energy and particles connects such an excitation with a similar excitation at neighboring lattice sites, so they are unable to migrate spontaneously.

The fact that numerically found excitations are very similar in shape to these cp excitations shows their statistical nature that has been studied in detail in [9]. Excitations constantly interact with surrounding low-amplitude waves, which leads to growth or preservation of their height when the energy of the waves is positive, while they decay in an environment of negative-energy waves. Hence, this formation or destruction of excitations depends on the sign of the total energy and it increases the system's entropy. The thermodynamic potentials of waves with a positive energy drive the excitations towards the central-peak state that absorbs a maximum amount of energy using a minimum amount of particles. This thermodynamic force of the wave-background is responsible for the local conservation of energy and particles in the excitation, which results in the pinning of the excitation.

On the other side, the interaction between waves and the excitation also leads to fluctuations of these quantities which can allow the excitation to migrate to a neighboring lattice site. If the surrounding waves have a sufficiently high amplitude, the fluctuations can allow the excitation to follow a migrational path on which the two quantities are not conserved locally. Such a migration is caused by a random process, and it ends when the excitation is again entangled at its new location by its high energy.

This can be used to trigger a migration externally. Three mechanisms for this have been discussed: Either, the phase or the amplitude of the acceptor can be changed, or a low-amplitude soliton can be brought to a collision with the excitation. The main point of these switching mechanisms is that they decrease the ratio of energy per particle and that they set the trajectory at the starting point of a heteroclinic connection between the donor and the acceptor site.


[1] V.M.Kenkre, D.K.Campbell,Phys.Rev.B 34, 4959 (1986)
[2] S.Aubry, G.Kopidakis, A.M.Morgante, G.P.Tsironis, Physica B 296, 222 (2001)
[3] Y.S.Kivshar, D.K.Campbell, Phys.Rev.E 48, 3077 (1993)
[4] A.B.Aceves, C.De Angelis, G.G.Luther, A.M.Rubenchik, S.K.Turitsyn, Physica D 87, 262 (1995)
A.B.Aceves, C.DeAngelis, T.Peschel, R.Muschall, F.Lederer, S.Trillo, S.Wabnitz, Phys.Rev.E 53. 1172 (1996)
[5] H.S.Eisenberg, Y.Silberberg, R.Morandotti, A.R.Boyd, J.S.Aitchison Phys.Rev.Lett.81,3383 (1998)
R.Morandotti, U.Peschel, J.S.Aitchison, H.S.Eisenberg, Y.Silberberg, Phys.Rev.Lett.83, 2726 (1999)
[6] R.S.MacKay, S.Aubry, Nonlinearity 7, 1623 (1994)
[7] S.Flach, C.R.Willis, Phys.Rev.Lett. 72, 1777 (1994)
[8] B.Rumpf, A.C.Newell, Phys.Rev.Lett. 87, 054102 (2001)
B.Rumpf,A.C.Newell, Physica D 184, 162 (2003)
B.Rumpf,A.C.Newell, Phy.Rev.E, in press,
online: http://arxiv.org/ps/nlin.CD/031259
[9] B.Rumpf, Phys.Rev.E, in press,
online: http://arxiv.org/ps/nlin.PS/031258
[10] R.A.Vicencio, M.I.Molina, Y.S.Kivshar, Optics Letters 28, 1942 (2003)